Immunization strategies for epidemic processes in time-varying contact networks

(Article begins on next page)

Immunization strategies for epidemic processes in time-varying contact networks

Michele Starnini[a], Anna Machens[b,c], Ciro Cattuto[d], Alain Barrat[b,c,d], Romualdo Pastor-Satorras[a]

[a]*Departament de Física i Enginyeria Nuclear, Universitat Politècnica de Catalunya, Campus Nord B4, 08034 Barcelona, Spain*
[b]*Aix Marseille Université, CNRS, CPT, UMR 7332, 13288 Marseille, France*
[c]*Université de Toulon, CNRS, CPT, UMR 7332, 83957 La Garde, France*
[d]*Data Science Laboratory, ISI Foundation, Torino, Italy*

Abstract

Spreading processes represent a very efficient tool to investigate the structural properties of networks and the relative importance of their constituents, and have been widely used to this aim in static networks. Here we consider simple disease spreading processes on empirical time-varying networks of contacts between individuals, and compare the effect of several immunization strategies on these processes. An immunization strategy is defined as the choice of a set of nodes (individuals) who cannot catch nor transmit the disease. This choice is performed according to a certain ranking of the nodes of the contact network. We consider various ranking strategies, focusing in particular on the role of the training window during which the nodes' properties are measured in the time-varying network: longer training windows correspond to a larger amount of information collected and could be expected to result in better performances of the immunization strategies. We find instead an unexpected saturation in the efficiency of strategies based on nodes' characteristics when the length of the training window is increased, showing that a limited amount of information on the contact patterns is sufficient to design efficient immunization strategies. This finding is balanced by the large variations of the contact patterns, which strongly alter the importance of nodes from one period to the next and therefore significantly limit the efficiency of any strategy based on an importance ranking of nodes. We also observe that the efficiency of strategies that include an element of randomness and are based on temporally local information do not perform as well but are largely independent on the amount of information available.

Keywords: Time-varying contact networks, Epidemic spreading, Immunization strategies

1. Introduction

The topology of the pattern of contacts between individuals plays a fundamental role in determining the spreading patterns of epidemic processes (Keeling and Eames, 2005). The first predictions of classical epidemiology (Anderson and May, 1992; Keeling and Rohani, 2008) were based on the homogeneous mixing hypothesis, assuming that all individuals have the same chance to interact with other individuals in the population. This assumption and the corresponding results were challenged by the empirical discovery that the contacts within populations are better described in terms of networks with a non-trivial structure (Newman, 2010). Subsequent studies were devoted to understanding the impact of network structure on the properties of the spreading process. The main result obtained concerned the large susceptibility to epidemic spread shown by networks with a strongly heterogeneous connectivity pattern, as measured by a heavy-tailed degree distribution $P(k)$ (defined as the probability distribution of observing one individual connected to k others) with a a diverging second moment (Pastor-Satorras and Vespignani, 2001; Lloyd and May, 2001; Newman, 2002; Moreno et al., 2002).

The original studies considered the interaction networks as static entities, in which connections are frozen or evolve at a time scale much longer than the one of the epidemic process. This static view of interaction networks hides however the fact that connections appear, disappear, or are rewired on various timescales, corresponding to the creation and termination of relations between pairs of individuals (Holme and Saramäki, 2012). Longitudinal data has traditionally been scarce in social network analysis, but, thanks to recent technological advances, researchers are now in a position to gather data describing the contacts in groups of individuals at several temporal and spatial scales and resolutions.

The analysis of empirical data on several types of human interactions (corresponding in particular to phone communications or physical proximity) has unveiled the presence of complex temporal patterns in these systems (Hui et al., 2005; Holme, 2005; Onnela et al., 2007; Cattuto et al., 2010; Tang et al., 2010; Stehlé et al., 2011a; Miritello et al., 2011; Karsai et al., 2011; Holme and Saramäki, 2012). In particular, the heterogeneity and burstiness of the contact patterns are revealed by the study of the distribution of the durations of contacts between pairs of agents, the distribution of the total time in contact of pairs of agents, and the distribution of gap times between two consecutive interactions involving a common individual. All these distributions are indeed heavy-tailed (often compatible with power-law behaviors), which corresponds to the burstiness of human interactions (Barabási, 2005).

These findings have led to a large modeling effort (Scherrer et al., 2008; Hill and Braha, 2010; Gautreau et al., 2009; Stehlé et al., 2010; Zhao et al., 2011; Perra et al., 2012; Starnini et al.,

2013) and stimulated the study of the impact of a network's dynamics on the dynamical processes taking place on top of it. The processes studied in this context include synchronization (Fujiwara et al., 2011), percolation (Parshani et al., 2010; Bajardi et al., 2012), social consensus (Baronchelli and Díaz-Guilera, 2012), or diffusion (Starnini et al., 2012). Epidemic-like processes have also been explored, both using realistic and toy models of propagation processes (Rocha et al., 2011; Isella et al., 2011; Stehlé et al., 2011a; Karsai et al., 2011; Miritello et al., 2011; Kivela et al., 2012; Panisson et al., 2012; Holme, 2013; Rocha and Blondel, 2013; Masuda and Holme, 2013). The study of simple schematic spreading processes over temporal networks helps indeed expose several properties of their dynamical structure: dynamical processes can in this context be conceived as probing tools of the network's temporal structure (Karsai et al., 2011).

The study of spreading patterns on networks is naturally complemented by the formulation of vaccination strategies tailored to the specific topological (and temporal) properties of each network. Optimal strategies shed light on how the role and importance of nodes depend on their properties, and can yield importance rankings of nodes. In the case of static networks, this issue has been particularly stimulated by the fact that heterogeneous networks with a heavy-tailed degree distribution have a very large susceptibility to epidemic processes, as represented by a vanishingly small epidemic threshold. In such networks, the simplest strategy consisting in randomly immunizing a fraction of the nodes is ineffective. More complex strategies, in which nodes with the largest number of connections are immunized, turn out to be effective (Pastor-Satorras and Vespignani, 2002) but rely on the global knowledge of the network's topology. This issue is solved by the so-called acquaintance immunization (Cohen et al., 2003), which prescribes the immunization of randomly chosen neighbors of randomly chosen individuals.

Few works have addressed the issue of the design of immunization strategies and their respective efficiency in the case of dynamical networks (Lee et al., 2012; Tang et al., 2011; Takaguchi et al., 2012; Masuda and Holme, 2013). In particular, Lee et al. (2012) consider datasets describing the contacts occurring in a population during a time interval $[0, T]$; they define and study strategies that use information from the interval $[0, \Delta T]$ to decide which individuals should be immunized in order to limit the spread during the remaining time $[\Delta T, T]$. Specifically, the authors introduce two strategies, called *Weight* and *Recent*. In the Weight strategy, a fraction f of nodes is selected at random: for each of these nodes, his/her most frequent contact in the interval $[0, \Delta T]$ is immunized. In the Recent strategy, the last contact before ΔT of each of the randomly chosen individuals is immunized. Both strategies are defined in the spirit of the acquaintance immunization, insofar as they select nodes using only partial (local) information on the network. Using a large $\Delta T = 75\% T$, Lee et al. (2012) show that these strategies perform better than random immunization and show that this is related to the temporal correlations of the dynamical networks.

In this paper, we investigate several immunization strategies

in temporal networks, including the ones considered by Lee et al. (2012), and address in particular the issue of the length ΔT of the "training window", which is highly relevant in the context of real-time, specific tailored strategies. The scenario we have in mind is indeed the possibility to implement a real-time immunization strategy for an ongoing social event, in which the set of individuals to the immunized is determined by strategies based on preliminary measurements up to a given time ΔT. The immunization problem takes thus a two-fold perspective: The specific rules (strategy) to implement, and the interval of time over which preliminary data are collected. Obviously, a very large ΔT will lead to more complete information, and a more satisfactory performance for most targeting strategies, but it incurs in the cost of a lengthy data collection. On the other hand, a short ΔT will be cost effective, but yield a smaller amount of information about the observed social dynamics.

In order to investigate the role of the training window length on the efficiency of several immunization strategies, we consider a simple snowball susceptible-infected (SI) model of epidemic spreading or information diffusion (Anderson and May, 1992). In this model, individuals can be either in the susceptible (S) state, indicating that they have not been reached by the "infection" (or information), or they can be in the infectious (I) state, meaning that they have been infected by the disease (or that they have received the information) and can further propagate it to other individuals. Infected individuals do not recover, i.e., once they transition to the infectious state they remain indefinitely in that state. Despite its simplicity, this model has indeed proven to provide interesting insights into the temporal structure and properties of temporal networks. Here we focus on the dynamics of the SI model over empirical time-varying social networks. The networks we consider describe time-resolved face-to-face contacts of individuals in different environments and were measured by the SocioPatterns collaboration (http://www.sociopatterns.org) using wearable proximity sensors (Cattuto et al., 2010). We consider the effect on the spread of an SI model of the immunization of a fraction of nodes, chosen according to different strategies based on different amounts of information on the contact sequence. We find a saturation effect in the increase of the efficiency of strategies based on nodes characteristics when the length of the training window is increased. The efficiency of strategies that include an element of randomness and are based on temporally local information do not perform as well but are largely independent on the amount of information available.

The paper is organized as follows: we briefly describe the empirical data in Sec. 2. In Sec. 3 we define the spreading model and some quantities of interest. The immunization strategies we consider are listed in Sec. 4. Sec. 5 contains the main numerical results, and we discuss in Sec. 6 and Sec. 7 the respective effects of temporal correlations and of randomness effects in the spreading model. Section 8 finally concludes with a discussion on our results.

2

2. Empirical contact sequences

We consider temporal networks describing the face-to-face close proximity of individuals in different contexts, collected by the SocioPatterns collaboration. We refer to http://www.sociopatterns.org and (Cattuto et al., 2010) for details on the data collection strategy, which is based on wearable sensors worn by individuals. The datasets give access, for each pair of participating individuals, to the list of time intervals in which they were in face-to-face close proximity ($\approx 1 - 2m$), with a temporal resolution of 20 seconds.

In this paper, we use temporal social networks measured in several different social contexts: the 2010 European Semantic Web Conference ("eswc"), a geriatric ward of a hospital in Lyon ("hosp"), the 2009 ACM Hypertext conference ("ht"), and the 2009 congress of the Société Francaise d'Hygiène Hospitalière ("sfhh"). These data correspond therefore to the fast dynamics of human contacts over the scale of a few days. A more detailed description of the corresponding contexts and analyses of these datasets can be found in (Cattuto et al., 2010; Van den Broeck et al., 2010; Isella et al., 2011; Stehlé et al., 2011b; Panisson et al., 2012). In Table 1 we summarize some of properties of the considered datasets.

3. Epidemic models and numerical methods

We simulate numerically the susceptible-infected (SI) spreading dynamics on the above describe datasets of human face-to-face proximity. The process is initiated by a single infected individual ("seed"). At each time step, each infected individual i infects with probability β the susceptible individuals j with whom i is in contact during that time step. The process stops either when all nodes are infected or at the end of the temporal sequence of contacts.

Different individuals have different contact patterns and *a priori* contribute differently to the spreading process. In order to quantify the spreading efficiency of a given node i, we proceed as follows: We consider i as the seed of the SI process, all other nodes being susceptible. We measure the half prevalence time, i.e., the time t_i needed to reach a fraction of infected nodes equal to 50% of the population. Since not all nodes appear simultaneously at $t = 0$ of the contact sequence, we define the *half-infection time* of seed node i as $T_i = t_i - t_{0,i}$,

Dataset	N	T	$\langle k \rangle$	$\langle s \rangle$	$\bar{f}$
eswc	173	4703	50	370	6.8
ht	113	5093	39	366	4.1
hosp	84	20338	30	1145	2.4
sfhh	416	3834	54	502	27.2

Table 1: Some properties of the SocioPatterns datasets under consideration: number of different individuals engaged in interactions (N); total duration of the contact sequence (T), measured in intervals of length $\Delta t = 20$ sec.; average degree $\langle k \rangle$ (number of different contacts) and average strength $\langle s \rangle$ (total time spent in face-to-face interactions) of the network of contacts aggregated over the whole sequence; average number of interactions $\bar{f}$ at each time step.
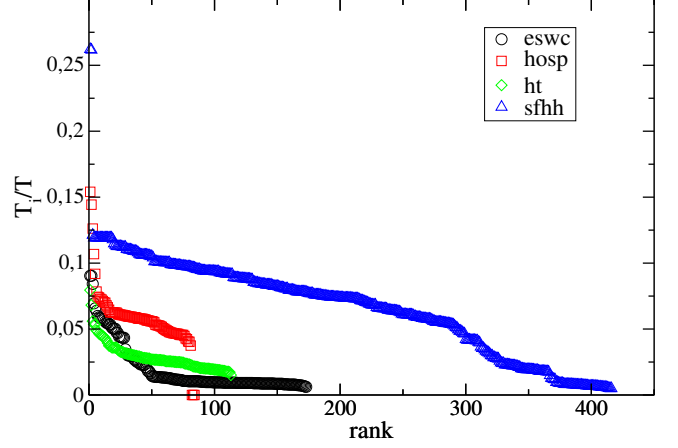

Figure 1: Rank plot of the half-infection times T_i divided by the contact sequence duration T for the various datasets.

where $t_{0,i}$ is the time at which node i first appears in the contact sequence. The half-infection time T_i can thus be seen as a measure of the spreading power of node i: smaller T_i values correspond to more efficient spreading patterns.

We first focus on the deterministic case $\beta = 1$ (the effects of stochasticity, as given by $\beta < 1$, are explored in Sec. 7). Figure 1 shows rank plot of the rescaled half-infection times T_i/T for various datasets, where T is the duration of the contact sequence. We note that T_i is quite heterogeneous, ranging from $T_i < 5\%T$ up to $T_i \simeq 20\%T$ [1].

Some nodes are therefore much more efficient spreaders than others. This implies that the immunization of different nodes could have very different impacts on the spreading process. To estimate this impact, we define for each node i the infection delay ratio τ_i as

$$\tau_i = \left\langle \frac{T_j^i - T_j}{T_j} \right\rangle_{j \neq i}, \tag{1}$$

where T_j^i is the half-infection time obtained when node j is the seed of the spreading process and node i is immunized, and the ratio is averaged over all possible seeds $j \neq i$ and over different starting times for the SI process (the half-infection time being much smaller than the total duration of the contact sequence, $T_j \simeq 0.1T$) [2]. The infection delay ratio τ_i quantifies therefore the average impact that the immunization of node i has on SI processes unfolding over the temporal network.

Figure 2 displays a rank plot of τ_i for various datasets. As expected, the immunization of a single node does most often lead to a limited delay of the spreading dynamics. Interestingly however, τ_i is broadly distributed and large values are also observed.

The infection delay ratio of a single node i, τ_i, can be generalized to the case of the immunization of any set of nodes

---

[1] We note that defining T_i as the time needed to reach a different fraction of the population, such as e.g. 25%, leads to a similar heterogeneity.

[2] Note that in some cases, node i is not present during the time window in which the SI process is simulated; in this case, $T_j^i = T_j$.
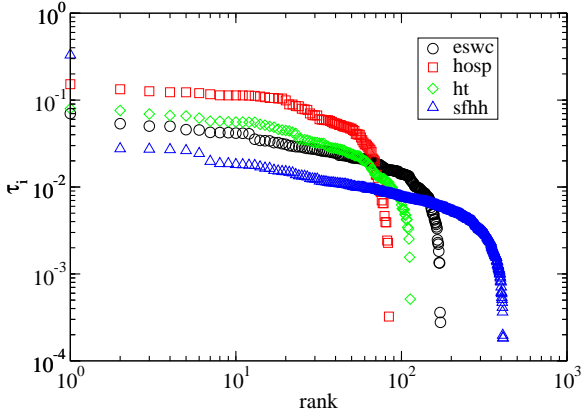
Figure 2: Rank plot of the infection delay ratio τ_i for various datasets.

$\mathcal{V} = \{i_1, \ldots, i_n\}$, with $n < N$. We measure the spreading slowing down obtained when immunizing the set $\mathcal{V}$ through the infection delay ratio

$$\tau_{\mathcal{V}} = \left\langle \frac{T_j^{\mathcal{V}} - T_j}{T_j} \right\rangle_{j \notin \mathcal{V}}, \qquad (2)$$

where $T_j^{\mathcal{V}}$ is the half-infection times of node j when all the nodes of set $\mathcal{V}$ are immunized, and the average is performed over all possible seeds $j \notin \mathcal{V}$ and different starting times for the SI process.

In addition to slowing down the propagation process, the immunization of certain individuals can also block the spreading paths towards other, non-immunized, individuals, limiting in this way the final number of infected individuals. We measure this effect through the *average outbreak size ratio*

$$i_{\mathcal{V}} = - \left\langle \frac{I_j^{\mathcal{V}} - I_j}{I_j} \right\rangle_{j \notin \mathcal{V}}, \qquad (3)$$

where $I_j^{\mathcal{V}}$ and I_j are the number of infected individuals (outbreak size) for an SI process with seed j, with and without immunization of the set $\mathcal{V}$, respectively. The ratio is averaged over all possible seeds $j \notin \mathcal{V}$ and over different starting times of the SI process.

4. Immunization strategies

An immunization strategy is defined by the choice of the set $\mathcal{V}$ of nodes to be immunized. We define here different strategies, and we compare their efficiencies in section 5 by measuring $\tau_{\mathcal{V}}$ and $i_{\mathcal{V}}$. More precisely, for each contact sequence of duration T we consider an initial temporal window $[0, \Delta T]$ over which various properties of nodes can be measured. A fraction f of the nodes, chosen according to different possible rules, is then selected and immunized (it forms the set $\mathcal{V}$). Finally, $\tau_{\mathcal{V}}$ and $i_{\mathcal{V}}$ are computed by simulating the SI process with and without immunization and averaging over starting seeds and times. For each selection rule, the two relevant parameters are

f and ΔT. Larger fractions f are naturally expected to lead to larger $\tau_{\mathcal{V}}$ and $i_{\mathcal{V}}$. Here we also consider the effect of ΔT, where a larger ΔT corresponds to a larger amount of information on the contact sequence. We investigate whether and how more information about the contact sequence yields a higher efficiency of the immunization strategy.

We consider the following strategies (or "protocols"):

K Degree protocol. We immunize the fN individuals with the highest aggregated degree in $[0, \Delta T]$ (Pastor-Satorras and Vespignani, 2002); the aggregated degree of an individual i corresponds to the number of different other individuals with whom i has been in contact during $[0, \Delta T]$;

BC Betwennness centrality protocol. We immunize the fN individuals with the highest betweenness centrality measured on the aggregated network in $[0, \Delta T]$ (Holme et al., 2002);

A Acquaintance protocol. We choose randomly an individual and immunize one of his contacts in $[0, \Delta T]$, repeating the process until fN individuals are immunized (Cohen et al., 2003);

W Weight protocol. We choose randomly an individual and immunize his most frequent contact in $[0, \Delta T]$, repeating for various elements until fN individuals are immunized (Lee et al., 2012);

R Recent protocol. We choose randomly an individual and immunize his last contact in $[0, \Delta T]$, repeating for various elements until fN individuals are immunized (Lee et al., 2012).

As a benchmark, we also consider the following two strategies:

Rn Random protocol. We immunize fN individuals chosen randomly among all nodes;

T τ-protocol. We immunize the first fN individuals with the highest τ_i, with τ_i calculated according to Eq. (1) in the interval $[0, \Delta T]$.

The **Rn** strategy uses no information about the contact sequence and we use it as a worst case performance baseline. The **T** strategy makes use, through the quantity τ_i, of the entire information about the contact sequence as well as complete information about the average effect of node immunization on SI processes taking place over the contact sequence. It could thus be expected to yield the best performance among all strategies.

The **A**, **W**, **R** and **Rn** strategies involve a random choice of individuals. In each of these cases, we average the results over 10^2 independent runs (each run corresponding to an independent choice of the individuals to immunize).

5. Numerical results

We first study the role of the temporal window ΔT on the efficiency of the various immunization strategies. To this aim,
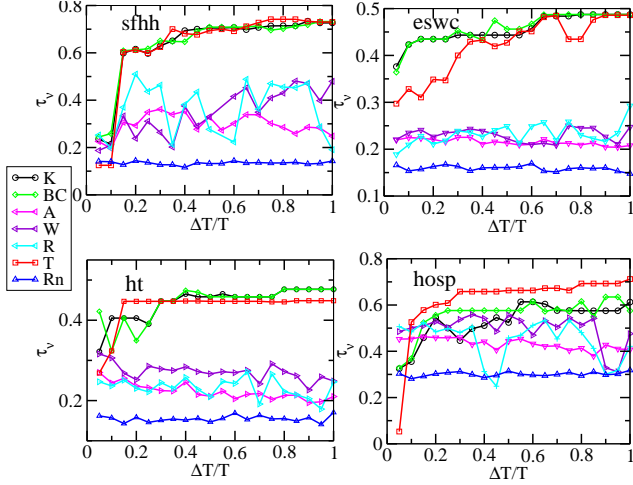
Figure 3: Infection delay ratio $\tau_{\mathcal{V}}$ as a function of the training window ΔT for different immunization protocols, for various datasets. The fraction of immunized individuals is $f = 0.05$.

Figure 4: Infection delay ratio $\tau_{\mathcal{V}}$ as a function of the training window ΔT for different immunization protocols, for various datasets. The fraction of immunized individuals is $f = 0.2$.

we consider two values of the fraction of immunized individuals, $f = 0.05$ and $f = 0.2$, and compute the infection delay ratio τ as a function of ΔT for each immunization protocol, and for each dataset. The results, displayed in Figs. 3 and 4, show that an increase in the amount of information available, as measured by an increase in ΔT, does not necessarily translate into an larger efficiency of the immunization, as quantified by the delay of the epidemic process. The **A**, **W** and **R** protocols have in all cases lower efficiencies that remain almost independent on ΔT. Moreover, and in contrast with the results of Lee et al. (2012) on a different dataset, **W** and **R** do not perform better than **A**. On the other hand, the immunization efficiency of the **K**, **BC** and **T** protocols increases at small ΔT and reaches larger values for all the datasets. As expected, the **Rn** protocol, which does not use any information, fares the worst. For $f = 0.05$, all protocols yield an infection delay ratio that is largely independent from ΔT for large enough training windows $\Delta T \gtrsim 0.2T$. For $f = 0.2$, the increase of τ is more gradual but tends to saturate for $\Delta T \gtrsim 0.4T$ as well. In all cases, a limited knowledge of the contact time series is therefore sufficient to estimate which nodes have to be immunized in order to delay the spreading dynamics, especially for small f, i.e., in case of limited resources. Interestingly, in some cases, the **K** and **BC** protocols lead to a larger delay of the spread than the **T** protocol, despite the fact that the latter is designed to explicitly identify the nodes which yield the maximal (individual) infection delay ratio. This could be ascribed to correlations between the activity patterns of nodes, leading to a non-linear dependence on f of the immunization efficiency (in particular, the list of nodes to immunize is built using the list of degrees, betweenness centralities, and τ_i values computed on the original network, without recomputing the rankings each time a node is removed).

Figure 5 reports the outbreak ratio $i_{\mathcal{V}}$ as a function of the temporal window ΔT for different vaccination protocols. Results similar to the case of the infection delay ratio are recovered: the reduction in outbreak size, as quantified by the average out-
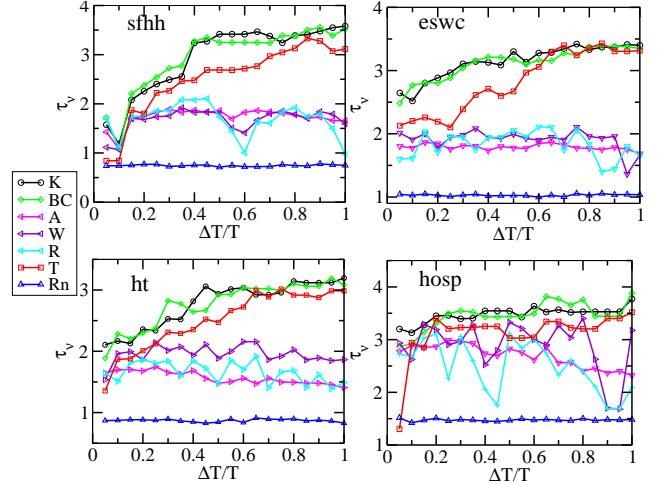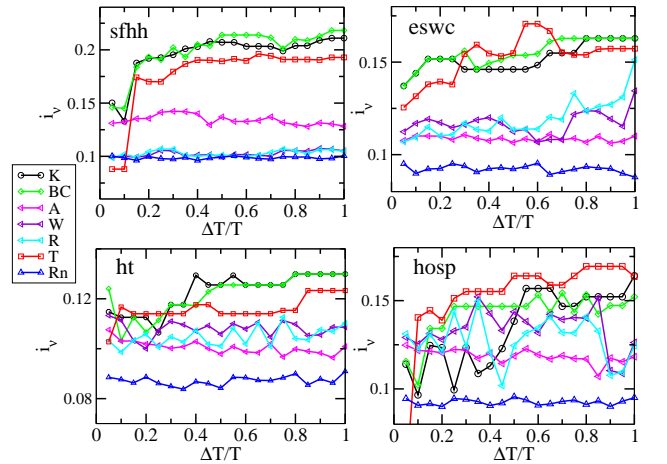

Figure 5: Average outbreak ratio $i_{\mathcal{V}}$ as a function of the temporal window ΔT for different vaccination protocols, for various datasets. Here the fraction of immunized nodes is $f = 0.05$.

break size ratio defined in Eq. (3), reaches larger values for the degree, betweenness centrality and **T** protocols than for the **A**, **W** and **R** protocols.

We finally investigate the robustness of our results when the fraction of immunized individuals varies. To this aim, we use a fixed length $\Delta T = 0.4T$ for the training window and we plot the infection delay ratio $\tau_{\mathcal{V}}$ and the average outbreak size ratio $i_{\mathcal{V}}$ as a function of f, respectively, in Figs. 6 and 7. The results show that the ranking of the strategies given by these two quantities is indeed robust with respect to variations in the fraction of immunized individuals. In particular, the **K** and **BC** protocols perform much better than the **W** and **R** protocols for at least one of the efficiency indicators.
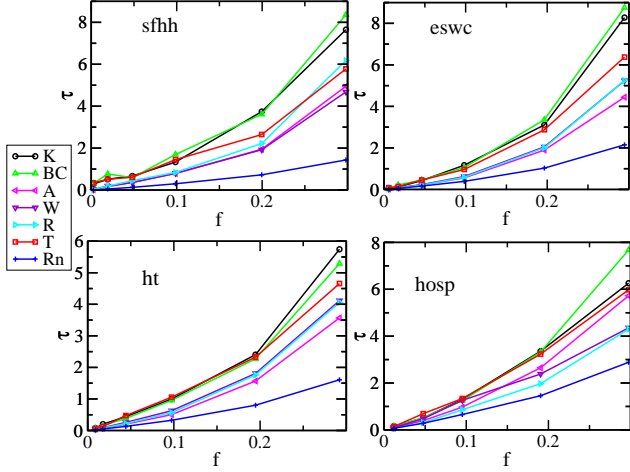
Figure 6: Infection delay ratio $\tau_{\mathcal{V}}$ as a function of the fraction f of immunized elements, for different vaccination protocols, for various datasets, and a fixed $\Delta T = 0.4T$.
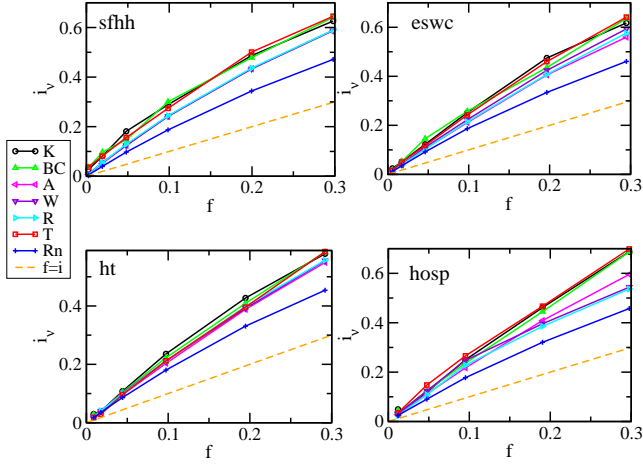

Figure 7: Average outbreak ratio $i_{\mathcal{V}}$ as a function of the fraction f of immunized elements, for different vaccination protocols, for various datasets. The dashed line represents the fraction of immunized individuals, f. Here $\Delta T = 0.4T$.

6. Effects of temporal correlations

Real time-varying networks are characterized by the presence of bursty behavior and temporal correlations, which impact the unfolding of dynamical processes (Holme, 2005; Kostakos, 2009; Isella et al., 2011; Nicosia et al., 2012; Bajardi et al., 2012; Holme and Saramäki, 2012; Starnini et al., 2012). For instance, if a contact between vertices i and j takes place only at the (discrete) times $\mathcal{T}_{ij} \equiv \{t_{ij}^{(1)}, t_{ij}^{(2)}, \cdots, t_{ij}^{(n)}\}$, it cannot be used in the course of a dynamical processes at any time $t \notin \mathcal{T}_{ij}$. A propagation process initiated at a given seed might therefore not be able to reach all the other nodes, but only those belonging to the seed's set of influence (Holme, 2005), i.e., those that can be reached from the seed by a time respecting path.

In order to investigate the role of temporal correlations, we consider a reshuffled version of the data in which correlations between consecutive interaction among individuals are re-
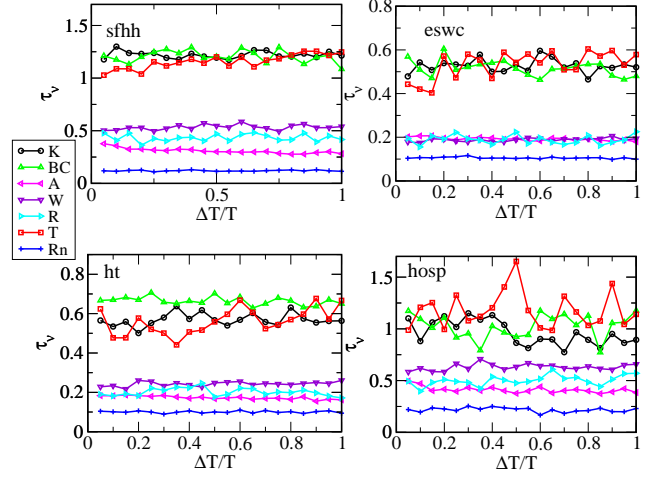

Figure 8: Infection delay ratio $\tau_{\mathcal{V}}$ as a function of the training window length ΔT, computed on one instance of a randomized dataset in which the time stamps of the contacts have been reshuffled, for different immunization protocols and various datasets, with $f = 0.05$.

moved. To this aim, we consider the list of events (i, j, t) describing a contact between i and j at time t and reshuffle at random their time stamps to build a synthetic uncorrelated new contact sequence. We then apply the same immunization protocols to this uncorrelated temporal network.

Figure 8 displays the corresponding results for the infection delay ratio $\tau_{\mathcal{V}}$ computed for SI spreading simulations performed on a randomized dataset (similar results are obtained for the average outbreak size ratio $i_{\mathcal{V}}$). We have checked that our results hold across different realizations of the randomization procedure. The efficiency of the protocol is then largely independent of the training window length. As the contact sequence is random and uncorrelated, all temporal windows are statistically equivalent, and no new information is added by increasing ΔT: in particular, as nodes appear in the randomly reshuffled sequence with a constant probability that depends on their empirical activity, the ranking of nodes according for instance to their aggregated degree remains very stable as ΔT changes, so that a very small ΔT is enough to reach a stable such ranking. Nevertheless, the efficiency ranking of the different protocols is unchanged: the degree, betweenness centrality, and $\mathbf{T}$ protocols outperform the other immunization strategies. Moreover, the efficiency levels reached are higher than for the original contact sequence: the correlations present in the data limit the immunization efficiency in the case of the present datasets. Note that studies of the role of temporal correlations on the speeding or slowing down of spreading processes have led to contrasting results, as discussed by Masuda and Holme (2013), possibly because of the different models and dataset properties considered.

7. Non-deterministic spreading

We also verify the robustness of our results using a probabilistic SI process with $\beta = 0.2$. We consider the same immu-
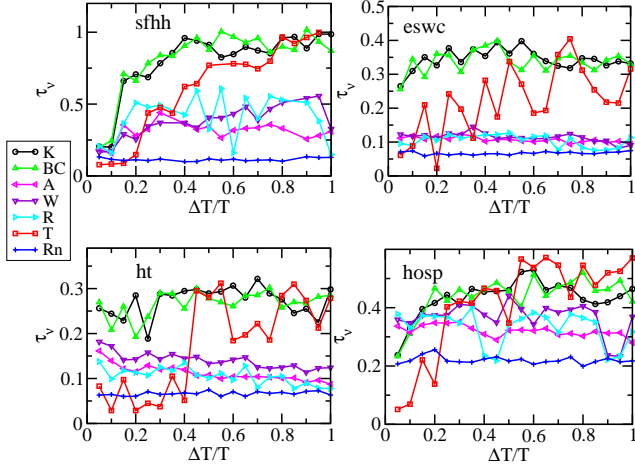
Figure 9: Infection delay ratio $\tau_\mathcal{V}$ as a function of the temporal window ΔT in a probabilistic SI with $\beta = 0.2$, for different vaccination protocols, various datasets, and $f = 0.05$.

Figure 10: Median degree *in the aggregated network* of the fraction $f = 0.05$ (red) and the $f = 0.2$ (black) nodes chosen by the **K** strategy at ΔT, vs $\Delta T/T$. The dashed horizontal lines mark the final values.

nization strategies and we compute the same quantities as in the case $\beta = 1$. Given the probabilistic nature of the spreading process, we now average the above observables over 10^2 realizations of the SI process. Figure 9 shows that our results hold in the case of a probabilistic epidemics spreading, although in this case the infection delay ratio $\tau_\mathcal{V}$ presents a noisy behavior, due to the stochastic fluctuations originated in the probabilistic spreading dynamics. The average outbreak ratio $i_\mathcal{V}$, not shown, behaves in a very similar way. Thus, also in this more realistic case with $\beta < 1$, a limited knowledge of the contact sequence is enough to identify which individuals to immunize.

8. Discussion

Within the growing body of work concerning temporal networks, few studies have yet considered the issue of immunization strategies and of their efficiency. In general terms, the amount of information that can be extracted from the data at hand about the characteristics of the nodes and links is a crucial ingredient for the design of optimal immunization strategies. Understanding how much information is needed in order to design good (and even optimal) strategies, and how the efficiency of the strategies depend on the information used, remain largely an open questions whose answer might depend on the precise dataset under investigation.

We have here leveraged several datasets describing contact patterns between individuals in varied contexts, and performed simulations in order to measure the effect of different immunization strategies on simple SI spreading processes. We have considered immunization strategies designed according to different principles, different ways of using information about the data, and different levels of randomness. Strategies range from the completely random **Rn** to the **A**, **W** and **R** strategies that include a random choice, to the fully deterministic **K**, **BC** and **T** that are based on various node's characteristics. Moreover, **K**
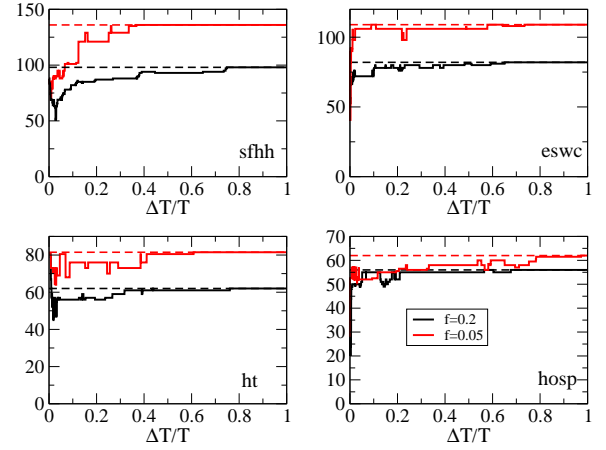
uses only local information while **BC** and **T** rely on the global knowledge of the connection patterns.

The strategies that are most efficient, as measured by the change in the velocity of the spread and by the final number of nodes infected, are the deterministic protocols, namely **K** and **BC**. Strategies based on random choices, even when they are designed in order to try to immunize "important" nodes, are less efficient.

We have moreover investigated how the performance of the various strategies depends on the time window on which the nodes' characteristics are measured. A longer time window corresponds indeed a priori to an increase in the available information and hence to the possibility to better optimize the strategies. We have found, however, a clear saturation effect in the efficiency increase of the various strategies as the training window on which they are designed increases. This is particularly the case when the fraction of immunized nodes is small (Fig. 3), for which a small ΔT is enough to reach saturation, while the saturation is more gradual for larger fractions of immunized (Fig. 4). Moreover, the strategies that involve a random component yield results that are largely independent on the amount of information considered.

In order to understand these results in more details, we have considered the evolution with time of the nodes' properties. In particular, we compare the largest degree nodes in the fully aggregated network with the set of nodes $\mathcal{S}_{\mathbf{K}}(\Delta T)$, chosen by following the **K** strategy on the training window $[0, \Delta T]$. To this aim, we show in Fig. 10 the median of the degrees, *in the fully aggregated network*, of the nodes of $\mathcal{S}_{\mathbf{K}}(\Delta T)$, as a function of ΔT. The median rapidly reaches its final value, showing that, even for short ΔT, the set of immunized nodes $\mathcal{S}_{\mathbf{K}}(\Delta T)$ has similar properties (here the degree) than what would be obtained by taking into account the whole dataset of length T.

Figure 11 moreover displays the evolution of the degree aggregated over the training window $[0, \Delta T]$, as a function of $\Delta T/T$, for several nodes. The fraction $f = 0.05$ of nodes with the largest degree in the fully aggregated network are ranked
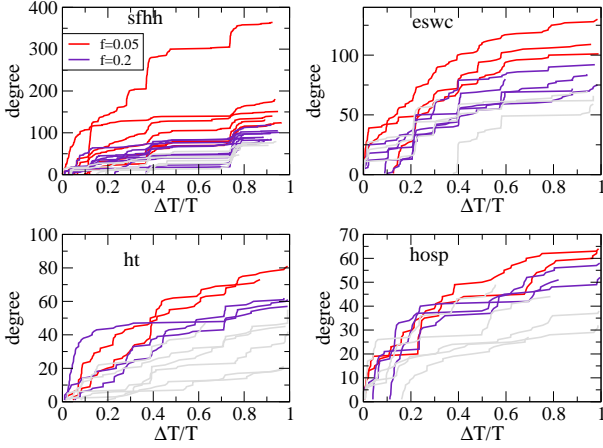
Figure 11: Degree of nodes on the network aggregated over ΔT, vs. $\Delta T/T$. The degrees of the fraction $f = 0.05$ nodes with highest degree on the fully aggregated network are shown in red (only every third node is shown for clarity). The degree of the nodes ranked between $0.05N$ and $0.2N$ in the fully aggregated network are shown in blue (only every sixth node is shown). The evolution of the aggregated degree of a small number of other nodes is shown in grey for comparison.

Figure 12: Degree of the several nodes on networks aggregated over temporal windows of 400 time steps $[t, t+400]$, vs t/T. The curves are colored according to the node's ranking in the network aggregated over $[0, T]$.

among the most connected nodes already for small training windows ΔT. For $f = 0.2$, the ranking fluctuates more and takes longer to stabilize. Overall, while the precise ordering scheme of the nodes according to their degree is not entirely stable with respect to increasing values of ΔT, a coarse ordering is rather rapidly reached: the nodes that reach a large degree at the end of the dataset are rapidly ranked among the highest degree nodes, and the nodes that in the end have a low degree are as well rapidly categorized as such. This confirms the result of Fig. 10 and explains why the **K** strategy reaches its best efficiency even at short training windows for small f, and with a more gradual saturation for larger fractions of immunized nodes.

The fact that high degree nodes are identified early on in the information collection process comes here as a surprise: for a temporal network with Poissonian events, all the information on the relative importance of links and nodes is present in the data as soon as the observation time is larger than the typical timescale of the dynamics; this is however a priori not the case for the bursty dynamics observed in real-world temporal networks. Various factors can explain the observed stability in the ranking of nodes. On the one hand, some nodes can possess some intrinsic properties giving them an important a priori position in the network (for instance, nurses in a hospital, or senior scientists in a conference) that ensure them a larger degree than other nodes even at short times. On the other hand, the stability of the ranking could in fact be only temporary, and due to the fact that nodes arriving earlier in the dataset have a larger probability to gather a large number of contacts. In this case, the observed stability of the ordering scheme could decrease for data collected on longer timescales.

Another reason for the saturation of the efficiency of the various strategies is shown in Fig. 12, which displays the evolution
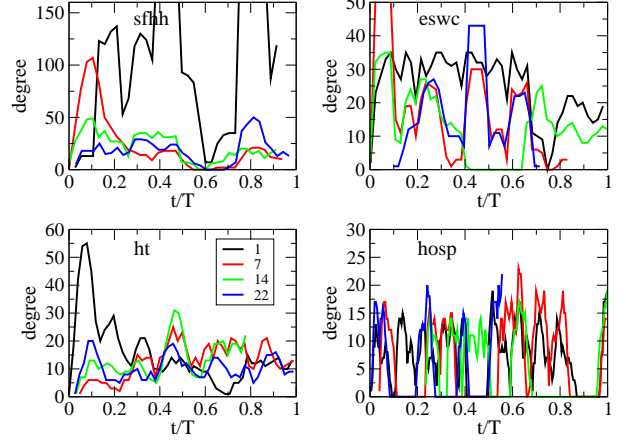
of the degree of some nodes in the network aggregated on a temporal window $[t, t + 400]$ versus t/T. This figure clearly shows that the importance of different nodes varies strongly depending on the initial time chosen for aggregation, and even a node with a large degree in the network aggregated on $[0, \Delta T]$ can have temporarily a small degree in a subsequent time window. The strong variation in the degree of nodes at different times clearly limits the efficiency not only of immunization strategies based on information that is local in time, but even of strategies based on aggregated information.

The main conclusion of our study is therefore twofold. On the one hand, a limited amount of information on the contact patterns is sufficient to design relevant immunization strategies; on the other hand, the strong variation in the contact patterns significantly limits the efficiency of any strategy based on importance ranking of nodes, even if such deterministic strategies still perform much better than the "recent" or "weight" protocols that are generalizations of the "acquaintance" strategy. Moreover, strategies based on simple quantities such as the aggregated degree perform as well as, or better, than strategies based on more involved measures such as the infection delay ratio defined in Sec. 3. We also note that, contrarily to the case investigated by Lee et al. (2012), the "recent" and "weight" strategies, which try to exploit the temporal structure of the data, do not perform clearly better than the simpler "acquaintance" strategy. Such apparent discrepancy might have various causes. In particular, Lee et al. (2012) consider spreading processes starting exactly at $t = \Delta T$ while we average over different possible starting times. The datasets used are moreover of different nature (Lee et al. (2012) indeed obtain contrasted results for different datasets) and have different temporal resolutions. A more detailed comparison of the different datasets' properties would be needed in order to fully understand this point, as discussed for instance by Masuda and Holme (2013).

8

9. Acknowledgments

References

Anderson, R.M., May, R.M., 1992. Infectious diseases in humans. Oxford University Press, Oxford.

Bajardi, P., Barrat, A., Savini, L., Colizza, V., 2012. Optimizing surveillance for livestock disease spreading through animal movements. Journal of The Royal Society Interface 9, 2814–2825.

Barabási, A., 2005. The origin of bursts and heavy tails in human dynamics. Nature 435, 207–211.

Baronchelli, A., Díaz-Guilera, A., 2012. Consensus in networks of mobile communicating agents. Phys. Rev. E 85, 016113.

Cattuto, C., Van den Broeck, W., Barrat, A., Colizza, V., Pinton, J.F., Vespignani, A., 2010. Dynamics of person-to-person interactions from distributed rfid sensor networks. PLoS ONE 5, e11596.

Cohen, R., Havlin, S., ben Avraham, D., 2003. Efficient immunization strategies for computer networks and populations. Phys. Rev. Lett. 91, 247901.

Fujiwara, N., Kurths, J., Díaz-Guilera, A., 2011. Synchronization in networks of mobile oscillators. Physical Review E 83, 025101.

Gautreau, A., Barrat, A., Barthélemy, M., 2009. Microdynamics in stationary complex networks. Proceedings of the National Academy of Sciences 106, 8847–8852.

Hill, S., Braha, D., 2010. A dynamic model of time-dependent complex networks. Phys. Rev. E 82, 046105.

Holme, P., 2005. Network reachability of real-world contact sequences. Phys. Rev. E 71, 046119.

Holme, P., 2013. Epidemiologically optimal static networks from temporal network data. preprint , arXiv:1302.0692.

Holme, P., Kim, B.J., Yoon, C.N., Han, S.K., 2002. Attack vulnerability of complex networks. Phys. Rev. E 65, 056109.

Holme, P., Saramäki, J., 2012. Temporal networks. Physics Reports 519, 97–125.

Hui, P., Chaintreau, A., Scott, J., Gass, R., Crowcroft, J., Diot, C., 2005. Pocket switched networks and human mobility in conference environments, in: WDTN '05: Proceedings of the 2005 ACM SIGCOMM workshop on Delay-tolerant networking, ACM, New York, NY, USA. pp. 244–251.

Isella, L., Stehlé, J., Barrat, A., Cattuto, C., Pinton, J.F., Van den Broeck, W., 2011. What's in a crowd? analysis of face-to-face behavioral networks. J. Theor. Biol 271, 166.

Karsai, M., Kivelä, M., Pan, R.K., Kaski, K., Kertész, J., Barabási, A.L., Saramäki, J., 2011. Small but slow world: How network topology and burstiness slow down spreading. Phys. Rev. E 83, 025102.

Keeling, M.J., Eames, K.T.D., 2005. Networks and epidemic models. J. R. Soc. Interface 2, 295–307.

Keeling, M.J., Rohani, P., 2008. Modeling Infectious Diseases in Humans and Animals. Princeton University Press, Princeton, N.J.

Kivela, M., Kumar Pan, R., Kaski, K., Kertesz, J., Saramaki, J., Karsai, M., 2012. Multiscale analysis of spreading in a large communication network. J. Stat. Mech. , P03005.

Kostakos, V., 2009. Temporal graphs. Physica A: Statistical Mechanics and its Applications 388, 1007 – 1023.

Lee, S., Rocha, L.E.C., Liljeros, F., Holme, P., 2012. Exploiting temporal network structures of human interaction to effectively immunize populations. PLoS ONE 7, e36439.

Lloyd, A.L., May, R.M., 2001. How viruses spread among computers and people. Science 292, 1316–1317.

Masuda, N., Holme, P., 2013. Predicting and controlling infectious disease epidemics using temporal networks. F1000Prime Reports 5, 6–.

Miritello, G., Moro, E., Lara, R., 2011. Dynamical strength of social ties in information spreading. Phys. Rev. E 83, 045102.

Moreno, Y., Pastor-Satorras, R., Vespignani, A., 2002. Epidemic outbreaks in complex heterogeneous networks. Eur. Phys. J. B 26, 521–529.

Newman, M.E.J., 2002. The spread of epidemic disease on networks. Phys. Rev. E 66, 016128.

Newman, M.E.J., 2010. Networks: An introduction. Oxford University Press, Oxford.

Nicosia, V., Tang, J., Musolesi, M., Russo, G., Mascolo, C., Latora, V., 2012. Components in time-varying graphs. Chaos 22, 023101.

Onnela, J.P., Saramäki, J., Hyvönen, J., Szabó, G., Lazer, D., Kaski, K., Kertész, J., Barabási, A.L., 2007. Structure and tie strengths in mobile communication networks. Proceedings of the National Academy of Sciences 104, 7332–7336.

Panisson, A., Barrat, A., Cattuto, C., Van den Broeck, W., Ruffo, G., Schifanella, R., 2012. On the dynamics of human proximity for data diffusion in ad-hoc networks. Ad Hoc Networks .

Parshani, R., Dickison, M., Cohen, R., Stanley, H.E., Havlin, S., 2010. Dynamic networks and directed percolation. EPL (Europhysics Letters) 90, 38004.

Pastor-Satorras, R., Vespignani, A., 2001. Epidemic spreading in scale-free networks. Phys. Rev. Lett. 86, 3200–3203.

Pastor-Satorras, R., Vespignani, A., 2002. Immunization of complex networks. Phys. Rev. E 65, 036104.

Perra, N., Gonçalves, B., Pastor-Satorras, R., Vespignani, A., 2012. Activity driven modeling of time varying networks. Nature Scientific Reports 2, srep00469.

Rocha, L.E.C., Blondel, V.D., 2013. Bursts of vertex activation and epidemics in evolving networks. PLoS Comput Biol 9, e1002974.

Rocha, L.E.C., Liljeros, F., Holme, P., 2011. Simulated epidemics in an empirical spatiotemporal network of 50,185 sexual contacts. PLoS Comput Biol 7, e1001109.

Scherrer, A., Borgnat, P., Fleury, E., Guillaume, J.L., Robardet, C., 2008. Description and simulation of dynamic mobility networks. Comp. Net. 52, 2842.

Starnini, M., Baronchelli, A., Barrat, A., Pastor-Satorras, R., 2012. Random walks on temporal networks. Phys. Rev. E 85, 056115.

Starnini, M., Baronchelli, A., Pastor-Satorras, R., 2013. Modeling human dynamics of face-to-face interaction networks. Physical Review Letters 110, 168701.

Stehlé, J., Barrat, A., Bianconi, G., 2010. Dynamical and bursty interactions in social networks. Phys. Rev. E 81, 035101.

Stehlé, J., Voirin, N., Barrat, A., Cattuto, C., Colizza, V., Isella, L., Régis, C., Pinton, J.F., Khanafer, N., Van den Broeck, W., Vanhems, P., 2011a. Simulation of an seir infectious disease model on the dynamic contact network of conference attendees. BMC Medicine 9.

Stehlé, J., Voirin, N., Barrat, A., Cattuto, C., Isella, L., Pinton, J.F., Quaggiotto, M., Van den Broeck, W., Régis, C., Lina, B., Vanhems, P., 2011b. High-resolution measurements of face-to-face contact patterns in a primary school. PLoS ONE 6, e23176.

Takaguchi, T., Sato, N., Yano, K., Masuda, N., 2012. Importance of individual events in temporal networks. New J. Phys. 14, 093003.

Tang, J., Mascolo, C., Musolesi, M., Latora, V., 2011. Exploiting temporal complex network metrics in mobile malware containment, in: Proceedings of IEEE 12th International Symposium on a World of Wireless, Mobile and Multimedia Networks (WOWMOM '11).

Tang, J., Scellato, S., Musolesi, M., Mascolo, C., Latora, V., 2010. Small-world behavior in time-varying graphs. Phys. Rev. E 81, 055101.

Van den Broeck, W., Cattuto, C., Barrat, A., Szomsor, M., Correndo, G., Alani, H., 2010. The live social semantics application: a platform for integrating face-to-face presence with on-line social networking, in: Proceedings of the 8th Annual IEEE International Conference on Pervasive Computing and Communications, p. 226.

Zhao, K., Stehlé, J., Bianconi, G., Barrat, A., 2011. Social network dynamics of face-to-face interactions. Phys. Rev. E 83, 056109.